JACS
JOURNAL OF THE AMERICAN CHEMICAL SOCIETY

Article

pubs.acs.org/JACS

In Vitro and *In Vivo* Enzyme Activity Screening via RNA-Based Fluorescent Biosensors for *S*-Adenosyl-L-homocysteine (SAH)

Yichi Su, Scott F. Hickey, Samantha G. L. Keyser, and Ming C. Hammond*

Department of Chemistry, University of California, Berkeley, California 94720, United States

Supporting Information

ABSTRACT: High-throughput enzyme activity screens are essential for target characterization and drug development, but few assays employ techniques or reagents that are applicable to both *in vitro* and live cell settings. Here, we present a class of selective and sensitive fluorescent biosensors for *S*-adenosyl-L-homocysteine (SAH) that provide a direct "mix and go" activity assay for methyltransferases (MTases), an enzyme class that includes several cancer therapeutic targets. Our riboswitch-based biosensors required an alternate inverted fusion design strategy, but retained full selectivity for SAH over its close structural analogue, the highly abundant methylation cofactor *S*-adenosyl-L-methionine (SAM). The level of ligand selectivity for these fluorescent biosensors exceeded that of commercial antibodies for SAH and proved critical to cellular applications, as we employed them to measure methylthioadenosine nucleosidase (MTAN) activity in live *Escherichia coli*. In particular, we were able to monitor *in vivo* increase of SAH levels upon chemical inhibition of MTAN using flow cytometry, which demonstrates high-throughput, single cell measurement of an enzyme activity associated with the biosynthesis of quorum sensing signal AI-2. Thus, this study presents RNA-based fluorescent biosensors as promising molecular reagents for high-throughput enzymatic assays that successfully bridge the gap between *in vitro* and *in vivo* applications.

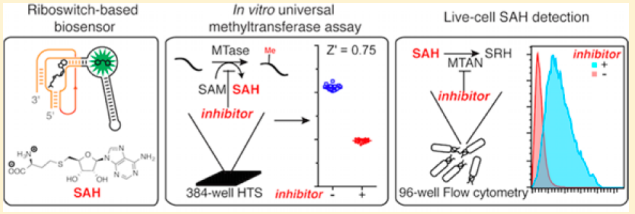

INTRODUCTION

Enzymes that produce or break down *S*-adenosyl-L-homocysteine (SAH) are important and emerging targets for cancer and infectious disease. As a stoichiometric byproduct, SAH is produced in all methyltransferase (MTase) reactions that use the universal cofactor *S*-adenosyl-L-methionine (SAM). Methylation of genomic DNA and associated histone proteins is one of the most widespread epigenetic modifications and affects control of gene regulation in all eukaryotic organisms, including humans. To date, DNA MTase inhibitors have been approved for treatment of myelodysplastic syndrome,[1] a bone marrow disease, and several protein MTases have been advanced as drug targets for treating mixed lineage leukemia,[2] non-Hodgkin lymphoma,[3] and other cancers.[4,5] Interestingly, SAH is competitively bound by MTases and acts as a strong product inhibitor because it only differs from SAM by a methyl group.[6] In the infectious disease area, SAH is a substrate for the enzyme 5′-methylthioadenosine nucleosidase (MTAN), which breaks down SAH in the biosynthesis of the quorum-sensing signal AI-2.[7] Thus, MTAN has been proposed as an attractive target for antibiotic development.[8]

Due to this growing interest in SAH-related enzymes for both basic research and biomedical studies, there is need for an efficient and high-throughput method for SAH detection both *in vitro* and *in vivo*. Currently, *in vitro* detection of SAH to assay MTase activity relies on processing SAH into chromogenic or fluorogenic derivatives.[9,10] However, involvement of additional enzyme reactions and reagents complicates assay development and risks high false-positive rates. Other methods of SAH detection include LC/MS-[11] and antibody-based[12] protocols, but they are either low-throughput or expensive to carry out. Commercial antibodies used in these assays exhibit only ∼180-fold selectivity for SAH over SAM.[12]

Indeed, detection of SAH in the cellular context is extremely challenging due to the low concentration of SAH compared to the high abundance of structurally related metabolites in the cell. For instance, SAH concentrations are in the low micromolar range in *Escherichia coli* lysates,[13] while related metabolites, such as SAM and ATP, have concentrations in the range from hundreds of micromolar to millimolar.[14] To our knowledge, there are no existing methods for directly monitoring SAH levels in live cells.

To address this challenge, we have generated a fluorescent biosensor that is highly selective for SAH. It was previously shown that a representative member of the SAH riboswitch class displays nanomolar binding affinity for SAH and effectively distinguishes between SAH and SAM by >1000-fold.[15] This remarkable degree of molecular discrimination made the riboswitch an attractive starting point for sensing applications. However, the architecture of the SAH riboswitch aptamer, which includes a 3′ terminal pseudoknot, precluded the use of existing design schemes for RNA-based fluorescent biosensors.[16−20]

Here, we describe the development of fluorescent biosensors that provide direct detection of SAH both *in vitro* and *in vivo*.

Received: February 19, 2016
Published: May 18, 2016

DOI: 10.1021/jacs.6b01621
J. Am. Chem. Soc. 2016, 138, 7040−7047

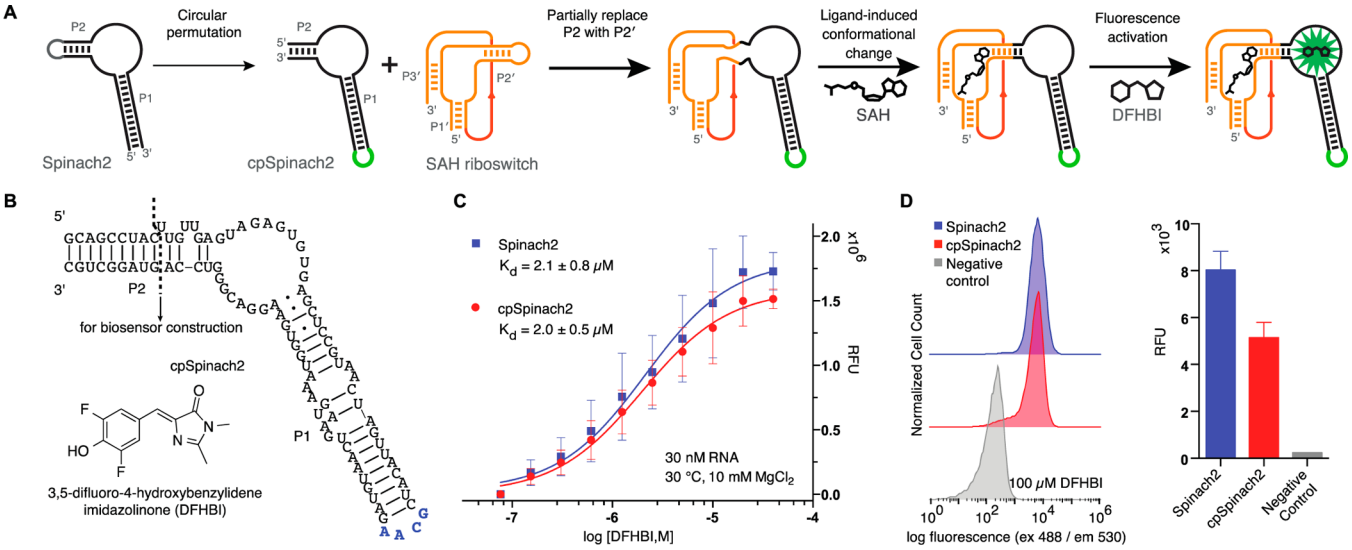

Figure 1. cpSpinach2 aptamer binds DFHBI and activates its fluorescence with similar performance to Spinach2 aptamer. (A) Circular permutation strategy enables the design of an SAH riboswitch-based fluorescent biosensor. Circular permutation of Spinach2 is achieved by removal of the P2 loop and addition of the P1 tetraloop (green). Fusion of cpSpinach2 with the SAH riboswitch (orange) via a P2/P2′ transducer stem generates the SAH biosensor. (B) Secondary structure model of cpSpinach2 and the chemical structure of DFHBI. (C) *In vitro* fluorescence activation and binding affinity measurements for RNA aptamers with DFHBI. (D) Live cell fluorescence measured by flow cytometry for *E. coli* BL21* cells expressing plasmid encoding RNA aptamers and incubated in media containing DFHBI. All error bars represent standard deviation between three independent replicates.

To incorporate a riboswitch aptamer with a 3′ terminal pseudoknot, we demonstrate an inverted fusion design to a circular permutant of the Spinach2 aptamer, cpSpinach2 (Figure 1A). The cpSpinach2 aptamer functions as a fluorophore-binding RNA with similar fluorescence turn-on properties as Spinach2. Using this design strategy and a phylogenetic screen of riboswitch sequences, we identified three fluorescent biosensors with high selectivity for SAH over SAM and affinities for SAH ranging from 75 nM to 1.3 μM. Using one of these SAH biosensors, we developed a "mix and go" fluorescent assay to measure the activities of DNA CpG MTase M.SssI and protein lysine MTase SET7/9. The reliability of the assay was demonstrated in a high-throughput format for substrate and inhibitor screens. Finally, we showcase the ability of these genetically encoded biosensors to monitor SAH levels *in vivo* by directly observing chemical inhibition of the endogenous enzyme MTAN in live *E. coli* cells.

RESULTS

cpSpinach2 as a Functional Alternative to the Spinach2 Aptamer. Prior strategies for construction of allosteric RNA-based fluorescent biosensors have taken advantage of the formation of a paired stem (P1′) by the 5′ and 3′ ends of the ligand-sensing aptamer domains.[17,18,20] However, structural studies of the SAH riboswitch aptamer showed that a 3′ pseudoknot forms part of the ligand-binding pocket,[21] which spaces the 5′ and 3′ ends considerably apart. Thus, to design an SAH biosensor, we envisioned an alternate design in which an internal paired stem (P2′) of the riboswitch aptamer could be used as the transducer stem to connect to the fluorophore-binding domain, the Spinach2 aptamer. However, fusion to Spinach2 would lead to a bipartite biosensor composed of two single-stranded RNAs. We reasoned that if a circular permutant of the Spinach2 aptamer was functional, we could generate an SAH biosensor via an inverted design (Figure 1A). As shown, the cpSpinach2 would be inserted internally in place of the natural P2 loop of the riboswitch aptamer, with a GCAA loop sequence added to link the original 5′ and 3′ ends (Figure 1B).

Circular permutations of functional RNAs are found in nature and have a rich history of application in structural and biochemical research of RNA.[22−25] However, the behavior of circularly permuted Spinach2 aptamer had not been examined previously. We first analyzed the dye binding and fluorescence activation of cpSpinach2 in comparison to Spinach2 *in vitro*. Following a previously reported method,[26] we derived the quantum yield (QY) and apparent dissociation constants (K_d) of the dye−aptamer complexes (Figure S1), which revealed that there was no significant difference in performance between the two aptamers under these conditions. Accordingly, the T_m values of Spinach2-DFHBI and cpSpinach2-DFHBI complexes also are similar, and reveal that the RNA−dye complexes have the same stability at 3 and 10 mM Mg^{2+}. A comparison to literature-reported[27] values of DFHBI−Spinach2 complexes is given in Table S1.

One caveat to the apparent K_d values determined above is that we have found that only a fraction of total RNA is functionally folded (~60% at 30 °C, Figure S2). Taking this into account, the corrected K_d values are closer to those determined by measuring fluorescence increase with titration of DFHBI to a solution containing the RNA aptamer at limiting concentrations (Figure 1C). It also should be noted that the K_d values are temperature sensitive, since a decrease in DFHBI binding affinity was observed for both aptamers when the assay was performed at higher temperature (37 °C) (Figure S3).

To compare the fluorescence of Spinach2 and cpSpinach2 in live cells, pET31b plasmids encoding the RNA aptamers in a tRNA scaffold were transformed into *E. coli* BL21* cells. Following IPTG induction of transcription, cells were incubated with DFHBI and fluorescence was quantitated by flow cytometry. The mean cellular fluorescence was measured as a function of increasing DFHBI concentration in the media

DOI: 10.1021/jacs.6b01621
J. Am. Chem. Soc. 2016, 138, 7040−7047

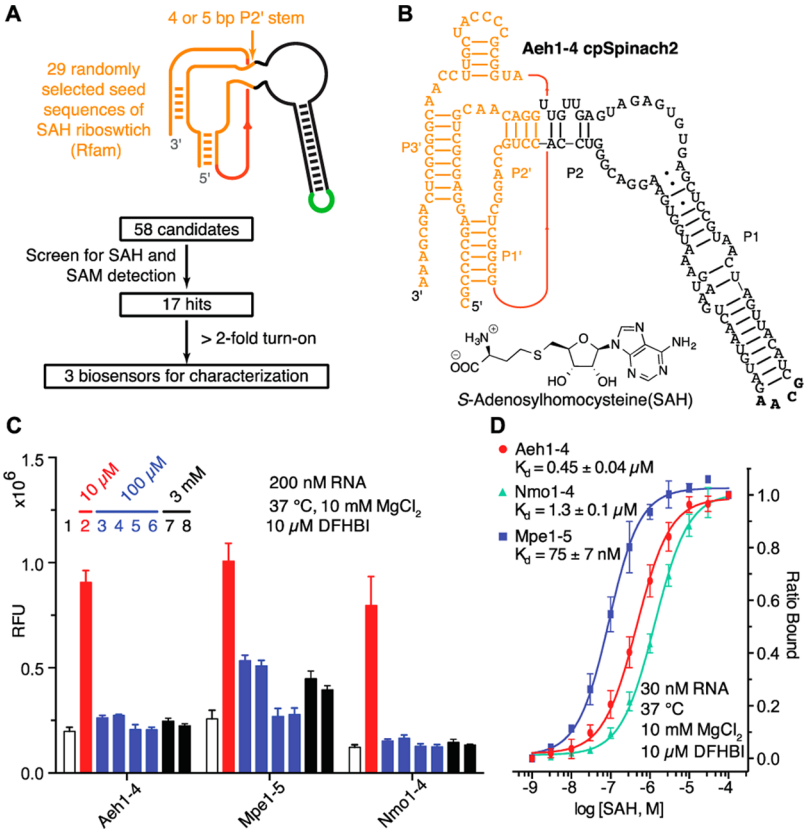

Figure 2. RNA-based fluorescent biosensors detect SAH selectively and with a range of binding affinities. (A) Design and work flow of screen for SAH riboswitch-based biosensors. (B) Secondary structure model of Aeh1−4 biosensor and chemical structure of SAH. (C) Ligand profile for SAH biosensors: 1, H_2O; 2, SAH; 3, SAM; 4, Adenosine; 5, D,L-homocysteine; 6, L-methionine; 7, ATP; 8, NAD+. (D) *In vitro* analysis of biosensor binding affinity for SAH. Fraction of biosensor bound was determined by normalizing to the fluorescence signal with saturating ligand (1.0) and without ligand (0). All error bars represent standard deviation of three independent replicates.

in order to determine the optimal conditions for aptamer fluorescence. Unexpectedly, full saturation of Spinach2 or cpSpinach2 fluorescence was not observed, even when *E. coli* cells were incubated in media containing up to 800 μM DFHBI (Figure S4). However, the nonspecific fluorescence signal increased when DFHBI concentration exceeded 100 μM. Thus, to balance higher fluorescence activation and lower nonspecific background, a concentration of 100 μM was adopted for further experiments. Under these conditions, cellular fluorescence activation for Spinach2 and cpSpinach2 was on average 34- and 22-fold over background, respectively (Figure 1D). Thus, cpSpinach2 is a functional alternative to Spinach2. It shows similar properties as Spinach2 *in vitro*, while it currently performs slightly less well in terms of fluorescence activation in live cells. This implies that some physiological factors, which are difficult to fully recapitulate *in vitro*, might affect its *in vivo* performance. For example, at 1 mM Mg^{2+}, cpSpinach2 only showed a slight decrease (0.5 °C) in T_m compared to Spinach2 *in vitro* (Table S1). However, since the T_m of both RNA−dye complexes are close to 37 °C, only ∼50% of the RNAs are well folded under cellular conditions, this small difference may lead to faster RNA turnover and thus amplify differences *in vivo*. Improvements are likely possible through directed mutagenesis for higher thermal stability, improved folding efficiency and less Mg^{2+} dependency.[28] Interestingly, this result also suggests that fully circular Spinach2 aptamers[29] or Spinach-based biosensors should retain activity.

Development and Characterization of RNA-Based Fluorescent Biosensors for SAH. We have found that sampling the phylogenetic diversity of riboswitch sequences can lead to improved biosensors.[30] Thus, 29 representatives were randomly selected from the seed sequences of the SAH riboswitch family deposited in Rfam,[31] and the P2′ loops were replaced with cpSpinach2 (Figures 2A,B, and S5). The natural P2′ stems are longer than 4 base pairs, but were truncated to 4 or 5 base pairs. Empirically, this design has been optimal for other Spinach2-based fluorescent biosensors that we have developed.[18,20] In this way, we constructed 58 biosensor candidates and screened them for fluorescence activation upon addition of SAH or SAM (Figures 2A and S6). In this initial screen, 17 of the putative biosensors showed selective fluorescence response to SAH.

Further analysis was performed on the three hits that showed more than 2-fold fluorescence activation in the screen. These biosensors incorporated SAH riboswitches from *Alkalilimnicola ehrlichii*, *Methylibium petroleiphilum*, and *Nitrococcus mobilis* and were called Aeh1−4, Mpe1−5, and Nmo1−4, respectively. The effects of varying Mg^{2+} and DFHBI concentrations on these biosensors were analyzed. Fluorescence turn-on of Aeh1−4 was highly Mg^{2+}-dependent, while Nmo1−4 and Mpe1−5 were much less affected by Mg^{2+} concentration (Figure S7). Decreasing DFHBI concentrations uniformly improved fluorescence turn-on of SAH biosensors, but led to overall decrease in fluorescence signal (Figure S8). Regardless, the biosensors are uniformly selective for SAH over related metabolites,

DOI: 10.1021/jacs.6b01621
J. Am. Chem. Soc. 2016, 138, 7040−7047

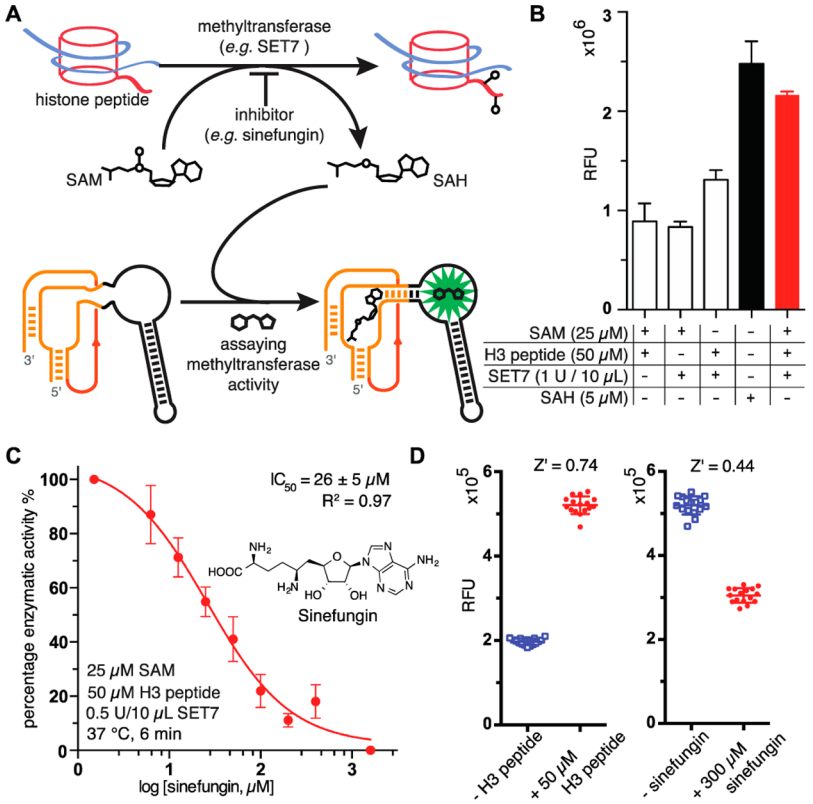

Figure 3. RNA-based fluorescent biosensors enable high-throughput screening of MTase activity and inhibition. (A) Schematic of MTase enzyme reaction and subsequent detection of SAH by fluorescent biosensors. (B) Aeh1−4 biosensor detects methylation activity of protein lysine MTase SET7/9 (red). Enzyme reactions that lack one component served as negative controls (white) and SAH served as a positive control (black). (C) Sinefungin inhibition of MTase SET7/9 is measured using Aeh1−4. Percent enzyme activity was determined by normalizing to the fluorescence signal without inhibitor (100%) and without substrate (0%). (D) The Z′ scores for MTase activity and inhibition assays using Aeh1−4 were determined in 384-well format. Error bars represent standard deviation of three independent replicates (B and C) or 16 replicates (D).

though a slight response of Mpe1−5 to high concentration of SAM or other adenine containing metabolites (adenosine, adenosine 5′-triphosphate (ATP) or β-nicotinamide adenine dinucleotide (NAD+)) was observed (Figure 2C). Further analysis showed that low micromolar SAH was sufficient to saturate fluorescence of the biosensors, while SAM needed to be at 1000- or 3000-fold higher concentrations to induce similar fluorescence response (Figure S9). This observation matches our expectation that these biosensors, like others we have made, retain the high selectivity of the original riboswitch aptamer, which was measured for one representative sequence to be >1000-fold.[15] It should be noted that we made these measurements after performing HPLC purification of the commercial SAM sample, which contained ∼2−3% of SAH (Figure S10). Our following success in employing the biosensors *in vivo* further support that the selectivity is at least 1000-fold. The combined suite of three biosensors have a dynamic range that spans 3 orders of magnitude for detection of SAH, from tens of nanomolar to tens of micromolar.

***In Vitro* Application of Fluorescent Biosensors toward a Universal High-Throughput MTase Activity Assay.** Next, we investigated using riboswitch-based biosensors for the development of high-throughput MTase activity assays (Figure 3A). As shown, enzymatic reactions were performed, then a fixed aliquot of the reaction mixture was diluted into the assay reaction containing the RNA biosensor, DFHBI, and buffer. The bacterial DNA MTase M.SssI possesses robust enzymatic activity and shares structural similarities with human DNA MTase 1 (DNMT1), an important epigenetic regulator and drug target.[32,33] With the use of any of the fluorescent biosensors, M.SssI activity was detected as an increase in fluorescence only in the presence of both SAM and dsDNA substrate (Figure S11). To determine the generality of the strategy, we also tested this assay on a histone protein MTase. Protein lysine MTases are of great interest in epigenetic and pharmaceutical research, but they have lower turnover rates than DNA MTases, which makes them harder to assay.[6] With the exception of DOT1L, all protein lysine MTases harbor a conserved domain (SET) for methylation; therefore, SET domain-containing MTase 7/9 (SET7/9) has been established as a model MTase.[6,34] As shown, the Aeh1−4 biosensor displayed a fluorescence response to SET7/9 activity, although signal-to-noise was lowered by increased background fluorescence in the control without SAM (Figure 3B). Such increased background might be due to incomplete removal of SAM or SAH during the purification of commercial SET7/9 MTase. These results show that MTase activity can be detected by RNA-based biosensors in a simple "mix and go" format with read-out in a fluorescence plate reader.

Activity assays using SAH biosensors also may allow for characterization and discovery of inhibitors of clinically relevant MTases. Sinefungin, a structural analogue of SAM, is a broad-spectrum MTase inhibitor that competes with SAM in the cofactor-binding pocket.[35] Previous work has shown that sinefungin has a similar binding affinity to SET7/9 as SAM, with an IC_{50} close to the starting concentration of SAM.[36]

DOI: 10.1021/jacs.6b01621
J. Am. Chem. Soc. 2016, 138, 7040−7047

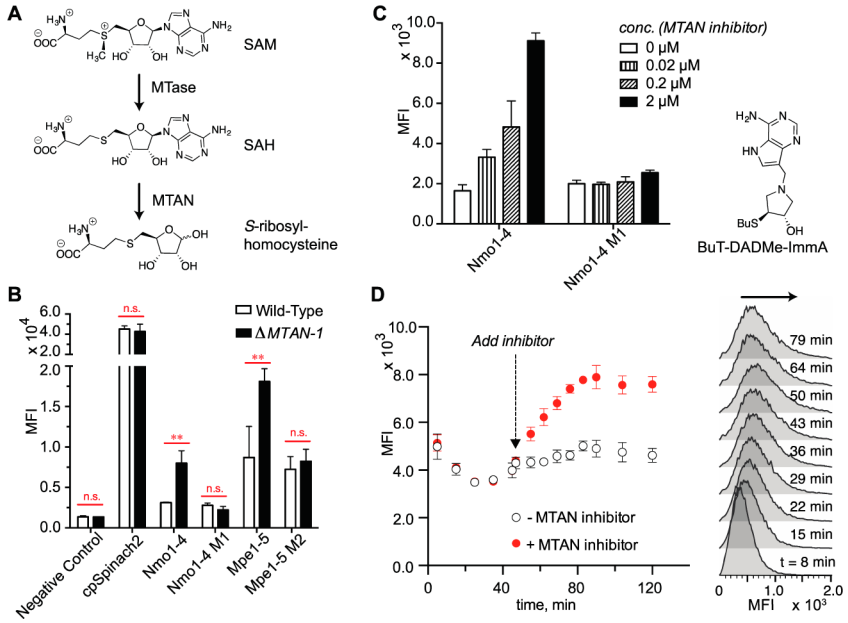

Figure 4. Detection of SAH in live *E. coli* by RNA-based fluorescent biosensors. (A) SAH is catabolized by the MTAN enzyme in *E. coli*. (B) Nmo1−4 and Mpe1−5 fluorescent biosensors detect accumulation of SAH in MTAN knockout strain compared to wild-type BL21* *E. coli*. MFI is mean fluorescence intensity of at least 20 000 live cells measured by flow cytometry (ex 488 nm, em 530 nm). Negative control is an inactive GFP mutant. n.s. is not significant; double asterik (**) indicates $p < 0.05$ by unpaired Student's two-tailed *t* test. (C) SAH accumulation caused by BuT-DADMe-ImmA inhibition of MTAN in wild-type *E. coli* BL21* cells is directly detected using Nmo1−4 biosensor. (D) Dynamic change of SAH levels in wild-type *E. coli* BL21* population with and without inhibitor treatment (1 μM) is measured using Nmo1−4. A set of representative flow cytometry profiles also is shown; the arrow indicates increase in mean fluorescence of the population. Error bars represent standard deviation of 3 (B, C) or 2 independent biological replicates (D).

Accordingly, we observed dose-dependent loss of fluorescence that corresponds to inhibition of SET7/9 by sinefungin (Figure 3C, Figure S12). The IC_{50} was determined to be 26 ± 5 μM, as expected given an initial SAM concentration of 25 μM (Figure 3C). When the initial concentration of SAM was increased to 40 μM, IC_{50} also increased to be 42 ± 16 μM (Figure S13), which confirmed the correlation between sinefungin and SAM.

All of the MTase activity and inhibition assays described above were performed in a 96-well plate and analyzed in a fluorescence plate reader. These conditions lend themselves to high-throughput screening (HTS), a format that would facilitate substrate and drug discovery for MTases of interest. To assess the statistical reliability and performance of HTS methods, a Z' score is commonly used, where a Z' score higher than 0.5 is considered to be excellent.[37] To calculate the Z' score for our activity and inhibition assays, 16 independent replicates of the methylation reactions were manually pipetted into a 384-well plate. The ability to identify substrates and inhibitors using these assays was assessed. With the use of the Aeh1−4 biosensor, the Z' score was 0.74 for the substrate screen and 0.44 for the inhibitor screen (Figure 3D). In the latter case, the lower Z' score is due to the biosensor signal not fully decreasing to background even at saturating inhibitor concentrations. We attribute this to sinefungin binding to the biosensor when used at high micromolar concentrations (Figure S14). Supporting this hypothesis, the higher affinity biosensor, Mpe1−5, has a Z' score of 0.81 for the substrate screen, but only 0.28 for the inhibitor screen, whereas the lower affinity biosensor, Nmo1−4, exhibited a desirable Z' score of 0.75 for the inhibitor screen (Figure S14). Overall, we have established a reliable and universal HTS assay for MTases using RNA-based biosensors.

***In Vivo* Application of Fluorescent Biosensors to Detect SAH in Live *E. coli* Cells.** Finally, the ability of these RNA-based biosensors to detect SAH in living cells was investigated. In *E. coli*, SAH is generated from SAM by cellular MTases and then metabolized by MTAN to form *S*-ribosylhomocysteine (Figure 4A). Another common SAH degradation pathway involves SAH hydrolase (SAHH), but *E. coli* lacks SAHH activity[38] and does not have any genes homologous to *Pseudomonas aeruginosa* SAHH. Knockout of the MTAN gene causes SAH accumulation to levels that are about 50-fold greater than those found in the wild-type *E. coli* MG1655 strain (1.3 μM for wild-type), while SAM levels remain relatively unaffected (0.4 mM).[13] To detect SAH accumulation, both *E. coli* BL21* wild-type and Δ*MTAN* cells expressing SAH biosensors in a tRNA scaffold were analyzed by flow cytometry. Nmo1−4 and Mpe1−5 were chosen for their greater fluorescence brightness and fluorescence turn-on at 37 °C and 3 mM Mg^{2+}, and their corresponding mutants, which disrupt the binding pocket and show no SAH response, were used as controls (Figure S15, Table S3). As expected, only the functional SAH biosensors exhibited significant increase in fluorescence signal in Δ*MTAN* versus wild-type cells (Figure 4B). A second Δ*MTAN* strain generated from a different target sequence also exhibited a similar trend for SAH detection (Figure S16). Because the Δ*MTAN* strain was observed to grow slower than wild-type, cpSpinach2 was also used to evaluate RNA expression; no significant difference in signal was observed for this control, consistent with results for the mutant biosensors. Furthermore, adenosine-2′,3′-dialdehyde (Adox), an inhibitor of SAH hydrolase, does not increase SAH biosensor fluorescence in *E. coli* cells (Figure S17), which is consistent with the previous observation that the enzyme activity was not detected in *E. coli*.[38]

DOI: 10.1021/jacs.6b01621
J. Am. Chem. Soc. 2016, 138, 7040−7047

Given the *in vitro* measured binding affinities for Nmo1−4 (0.75 μM) and Mpe1−5 (19 nM) (Figure S15), we had expected that in wild-type *E. coli* cells, Mpe1−5 should exhibit saturated fluorescence, while Nmo1−4 should show fluorescence turn-on. However, our observations (Figures 4B, S16) instead showed that SAH levels in wild-type *E. coli* BL21* cells are close to the middle of the detection range for Mpe1−5 and below the detection limit of Nmo1−4 (Figures 4B, S16). There are several possible explanations for our observations. First, our biosensors may have poorer binding affinities for SAH under physiological conditions, which are difficult to fully recapitulate *in vitro*. In fact, we found that the presence of 3 mM ATP in the *in vitro* binding reactions slightly reduced the apparent binding affinity of the biosensors for SAH (Figure S18A,B). This effect is likely due to some competitive binding of ATP to the SAH binding pocket, as the riboswitch aptamer has been previously shown to have weak affinity to ATP.[21] We found that 3 mM of NAD+, which had even weaker affinity to the riboswitch, had no effect on SAH binding affinity. The physiological concentrations of ATP and of NAD+ are 3−10 and 3 mM, respectively, in *E. coli*.[14,39]

Interestingly, the biosensors do not show fluorescence turn-on in direct response to ATP or NAD+. Mpe1−5 actually has lower fluorescence in the presence of 10 mM ATP (Figure S18C). We determined that this unexpected quenching effect is likely due to competitive binding of ATP to the DFHBI binding pocket, as the Spinach2 aptamer alone showed the same effect (Figure S18D). In fact, this result explains the discrepancy between the *in vitro* binding affinity measured for DFHBI and the inability to saturate fluorescence signal *in vivo* for Spinach2 and cpSpinach2 (Figure S4). Importantly, however, the fluorescence signals of Spinach2, cpSpinach2, and our biosensors are not fully quenched *in vivo*, which may reflect that free ATP concentrations are lower than 10 mM.

Another possible explanation is if the cellular concentration of biosensor is much higher than the actual K_d value (RNA sensor levels vary from 13.5 to 75 μM),[17] the signal becomes proportional to the amount of ligand up to saturation of the biosensor, rather than dependent on K_d. Due to these complicating factors, we caution that *in vitro* binding affinities cannot be directly extrapolated to interpret *in vivo* fluorescence readings. However, relative quantitation is possible when analyzing signal from a single biosensor, and our results also show that the relative affinities of different biosensors measured *in vitro* are consistent with their *in vivo* performance. Finally, the *in vivo* data further confirm that the selectivity of our biosensors for SAH over SAM is ∼1000-fold or greater, because little to no background fluorescence activation is observed even though cellular SAM concentrations are high.

We next attempted to monitor the dynamic change of SAH levels in live cells. For this purpose, BuT-DADMe-ImmA, a potent MTAN inhibitor developed by Schramm and co-workers,[8] was used to chemically regulate MTAN activity and thus SAH levels. In previous studies, this inhibitor showed a dose-dependent inhibition of MTAN in live *E. coli* cells with an IC_{50} of 125 nM, and 0.5 μM inhibitor reduced the MTAN activity to a level comparable to an MTAN knockout strain.[8] *E. coli* BL21* wild-type cells were grown overnight in the presence of various concentrations of MTAN inhibitor. These concentrations were shown to be not lethal to the bacteria.[8] Dose-dependent MTAN inhibition led to elevation of SAH levels as detected by Nmo1−4, while the mutant biosensor (Nmo1−4 M1) exhibited no fluorescence increase (Figure 4C). Importantly, our biosensors are highly selective for SAH and thus exhibit no fluorescence response to the MTAN inhibitor and little response to methylthioadenosine (MTA), the other substrate of MTAN, even at high micromolar concentrations (Figure S19). Thus, the dose-dependent fluorescence activation can be attributed to SAH accumulation in treated cells. Excitingly, we can observe gradual SAH accumulation in live cells upon inhibitor treatment, but flow cytometry analysis also reveals that the inhibition effect is not uniform, as the distribution of cellular fluorescence broadens with time (Figure 4D). Analysis of cpSpinach2 fluorescence under related conditions confirm that biosensor levels remain relatively constant during the time-course (Figure S20). Taken together, these results demonstrate the application of our biosensors in detecting and monitoring SAH levels in live *E. coli* cells.

DISCUSSION

Here, we reveal that cpSpinach2 provides a different scaffold for RNA tagging and biosensor design. Besides the SAH riboswitch, many other natural riboswitch and *in vitro* selected aptamers contain pseudoknots,[40−42] and they were thought to be incompatible with former biosensor designs.[19] Our results show that cpSpinach2 provides a way to overcome this issue.

With cpSpinach2 in hand, we developed a series of RNA-based biosensors for SAH. For these biosensors, the affinity for SAH is reduced relative to values reported for natural SAH riboswitch aptamers.[15] This may be partly due to differences in conditions for the assays. Also, the specific SAH riboswitch aptamers identified in our biosensor screen had not been previously characterized, nor had the effect of truncations of the P2 stem been evaluated. However, it should be noted that one of these first-generation biosensors, Mpe1−5, has an apparent binding affinity to SAH of 75 nM (Figure 2D), which effectively allows activity assays to be performed with low nanomolar concentrations of enzymes. Importantly, only under these assay conditions can one screen for high-affinity inhibitor compounds with low nanomolar dissociation constants, and the direct fluorescent read-out enables our assay to be reliable and high-throughput (Figure 3C,D). Furthermore, we applied fluorescent biosensors to analyze methyltransferase activity *in vitro*, and our assay exhibits comparable or better selectivity and fluorescence turn-on than commercial assays that require both an antibody and a fluorescent analogue of SAH (Table S2).[12]

Our results present RNA-based biosensors as a promising alternative reagent to antibodies, which are expensive to produce,[43] exhibit batch-to-batch variation,[44] and have less affinity or selectivity for small molecule compounds versus protein targets.[45] For example, the reported selectivity for a monoclonal antibody for SAH versus SAM was 180-fold,[12] whereas the riboswitch aptamer and corresponding biosensor have >1000-fold selectivity.[15] Our system benefits from ease of synthesis and purification, as the RNA-based biosensors are enzymatically synthesized from DNA templates (∼150 nts) *in vitro* in one step, and the profluorescent dye DFHBI is readily synthesized in three steps.[27] The direct "mix and go" format of our assay in detecting SAH is also advantageous over enzyme-coupled MTase assays.[6,9,46]

Another clear advantage of RNA-based biosensors over antibodies is that they can be employed to measure intracellular levels of a metabolite in live cells. Unlike prior examples,[17−20] in which high-abundance metabolites (SAM, ADP) or relatively specialized compounds (cyclic dinucleotides, TPP) were being detected, SAH posed a special challenge because it is very low

DOI: 10.1021/jacs.6b01621
J. Am. Chem. Soc. 2016, 138, 7040−7047

in abundance relative to the highly analogous cofactor SAM. It was further compelling to find a solution to this molecular recognition problem because of the importance of related enzymes as disease targets. The recent discovery that reversible RNA methylation is widespread in humans and other organisms[47−49] shows that more remains to be elucidated about the activity and function of enzymes associated with cellular methylation events. To our knowledge, no current method existed for *in vivo* monitoring of enzyme activity related to production of SAH in live cells.

Assay reagents that are applicable to both *in vitro* and live cell settings, like SNAP-tag protein-based biosensors,[50,51] are valuable tools for biomedical screen. However, such examples are very rare. Our work clearly demonstrates RNA-based biosensors as another promising example.

Furthermore, we have demonstrated high-throughput, single-cell monitoring of SAH levels using flow cytometry. Using an RNA-based fluorescent biosensor, we directly visualized accumulation of substrate (SAH) upon chemical inhibition of an enzyme (MTAN) in the context of living bacteria (Figure 4). The ability to monitor the effect of a drug on a population of bacteria in a high-throughput manner is an attractive application of our biosensors for medicinal chemistry research. We envision that in the future, it may be possible to use fluorescence-activated cell sorting (FACS) to evaluate the *in vivo* efficacy or mechanism of inhibitors, or to isolate population members that have become drug-resistant at different time points.

In summary, this work demonstrates proof-of-concept for *in vitro* biochemical assays and intracellular SAH detection with novel RNA-based SAH biosensors. We anticipate that for advanced applications, our first generation fluorescent biosensors require further improvements. Higher fold turn-on of fluorescence and binding affinity to both SAH and DFHBI would be generally desirable for biosensor performance and likely can be achieved via a broader phylogenetic screen and/or directed evolution. For development of high-throughput *in vitro* assays, biosensors should be screened for buffer compatibility. It would also be interesting to assess the effect of unnatural nucleotide modifications on biosensor function and resistance to RNase degradation.

For *in vivo* applications, higher thermal stability and reduced competitive binding to ATP, which is an issue for both Spinach2 and cpSpinach2, would lead to brighter cellular fluorescence signal. To this end, efforts to engineer new DFHBI-binding aptamers[52] or novel RNA-dye pairs will be important. Also, a ratiometric read-out would be desirable for single-cell signal normalization, affording more accurate quantitation of SAH *in cellulo*. Strategies like fusion of fluorogenic RNA aptamers or development of FRET biosensors are being actively explored. Our long-term goal is to develop next-generation fluorescent biosensors that can be used for targeted *in vivo* imaging of MTase activity.

■ ASSOCIATED CONTENT

Supporting Information

The Supporting Information is available free of charge on the ACS Publications website at DOI: 10.1021/jacs.6b01621.

Material and methods section, additional discussion, figures and tables (PDF)

■ AUTHOR INFORMATION

Corresponding Author

*mingch@berkeley.edu

Notes

The authors declare the following competing financial interest(s): The authors have filed a provisional patent application on fluorescent biosensors for SAH.

■ ACKNOWLEDGMENTS

We thank V. L. Schramm, Albert Einstein College of Medicine, G. B. Evans and P. C. Tyler, Ferrier Research Institute, Victoria University of Wellington for providing BuT-DADMe-ImmA. This work was supported in part by an NIH New Innovator Award (DP2 OD008677) to M.C.H., a Career Award at the Scientific Interface from the Burroughs Wellcome Fund to M.C.H., and a grant from Agilent Technologies as an industry partner of the Synthetic Biology Institute.

■ REFERENCES

(1) Fenaux, P.; Mufti, G. J.; Hellstrom-Lindberg, E.; Santini, V.; Finelli, C.; Giagounidis, A.; Schoch, R.; Gattermann, N.; Sanz, G.; List, A.; Gore, S. D.; Seymour, J. F.; Bennett, J. M.; Byrd, J.; Backstrom, J.; Zimmerman, L.; McKenzie, D.; Beach, C.; Silverman, L. R. *Lancet Oncol.* **2009**, *10* (3), 223.

(2) Daigle, S. R.; Olhava, E. J.; Therkelsen, C. A.; Basavapathruni, A.; Jin, L.; Boriack-Sjodin, P. A.; Allain, C. J.; Klaus, C. R.; Raimondi, A.; Scott, M. P.; Waters, N. J.; Chesworth, R.; Moyer, M. P.; Copeland, R. A.; Richon, V. M.; Pollock, R. M. *Blood* **2013**, *122* (6), 1017.

(3) Knutson, S. K.; Kawano, S.; Minoshima, Y.; Warholic, N. M.; Huang, K.-C.; Xiao, Y.; Kadowaki, T.; Uesugi, M.; Kuznetsov, G.; Kumar, N.; Wigle, T. J.; Klaus, C. R.; Allain, C. J.; Raimondi, A.; Waters, N. J.; Smith, J. J.; Porter-Scott, M.; Chesworth, R.; Moyer, M. P.; Copeland, R. A.; Richon, V. M.; Uenaka, T.; Pollock, R. M.; Kuntz, K. W.; Yokoi, A.; Keilhack, H. *Mol. Cancer Ther.* **2014**, *13* (4), 842.

(4) Dawson, M. A.; Kouzarides, T. *Cell* **2012**, *150* (1), 12.

(5) Wagner, T.; Jung, M. *Nat. Biotechnol.* **2012**, *30* (7), 622.

(6) Luo, M. *ACS Chem. Biol.* **2012**, *7* (3), 443.

(7) Parveen, N.; Cornell, K. A. *Mol. Microbiol.* **2011**, *79* (1), 7.

(8) Gutierrez, J. A.; Crowder, T.; Rinaldo-Matthis, A.; Ho, M.-C.; Almo, S. C.; Schramm, V. L. *Nat. Chem. Biol.* **2009**, *5* (4), 251.

(9) Dorgan, K. M.; Wooderchak, W. L.; Wynn, D. P.; Karschner, E. L.; Alfaro, J. F.; Cui, Y.; Zhou, Z. S.; Hevel, J. M. *Anal. Biochem.* **2006**, *350* (2), 249.

(10) Wang, R.; Ibáñez, G.; Islam, K.; Zheng, W.; Blum, G.; Sengelaub, C.; Luo, M. *Mol. BioSyst.* **2011**, *7* (11), 2970.

(11) Lakowski, T. M.; Frankel, A. *Anal. Biochem.* **2010**, *396* (1), 158.

(12) Graves, T. L.; Zhang, Y.; Scott, J. E. *Anal. Biochem.* **2008**, *373* (2), 296.

(13) Halliday, N. M.; Hardie, K. R.; Williams, P.; Winzer, K.; Barrett, D. a. *Anal. Biochem.* **2010**, *403* (1−2), 20.

(14) Bennett, B. D.; Kimball, E. H.; Gao, M.; Osterhout, R.; Van Dien, S. J.; Rabinowitz, J. D. *Nat. Chem. Biol.* **2009**, *5* (8), 593.

(15) Wang, J. X.; Lee, E. R.; Morales, D. R.; Lim, J.; Breaker, R. R. *Mol. Cell* **2008**, *29* (6), 691.

(16) Stojanovic, M. N.; Kolpashchikov, D. M. *J. Am. Chem. Soc.* **2004**, *126* (30), 9266.

(17) Paige, J. S.; Nguyen-Duc, T.; Song, W.; Jaffrey, S. R. *Science* **2012**, *335* (6073), 1194.

(18) Kellenberger, C. A.; Wilson, S. C.; Sales-Lee, J.; Hammond, M. C. *J. Am. Chem. Soc.* **2013**, *135* (13), 4906.

(19) You, M.; Litke, J. L.; Jaffrey, S. R. *Proc. Natl. Acad. Sci. U. S. A.* **2015**, *112* (21), E2756.

(20) Kellenberger, C. A.; Wilson, S. C.; Hickey, S. F.; Gonzalez, T. L.; Su, Y.; Hallberg, Z. F.; Brewer, T. F.; Iavarone, A. T.; Carlson, H. K.; Hsieh, Y.-F.; Hammond, M. C. *Proc. Natl. Acad. Sci. U. S. A.* **2015**, *112* (17), 5383.

DOI: 10.1021/jacs.6b01621
J. Am. Chem. Soc. 2016, 138, 7040−7047

(21) Edwards, A. L.; Reyes, F. E.; Héroux, A.; Batey, R. T. *RNA* **2010**, *16* (11), 2144.
(22) Pan, T.; Gutell, R. R.; Uhlenbeck, O. C. *Science* **1991**, *254* (5036), 1361.
(23) Nolan, J. M.; Burke, D. H.; Pace, N. R. *Science* **1993**, *261* (5122), 762.
(24) Pan, T.; Uhlenbeck, O. C. *Gene* **1993**, *125* (2), 111.
(25) Perreault, J.; Weinberg, Z.; Roth, A.; Popescu, O.; Chartrand, P.; Ferbeyre, G.; Breaker, R. R. *PLoS Comput. Biol.* **2011**, *7* (5), e1002031.
(26) Babendure, J. R.; Adams, S. R.; Tsien, R. Y. *J. Am. Chem. Soc.* **2003**, *125* (48), 14716.
(27) Paige, J. S.; Wu, K. Y.; Jaffrey, S. R. *Science* **2011**, *333* (6042), 642.
(28) Filonov, G. S.; Moon, J. D.; Svensen, N.; Jaffrey, S. R. *J. Am. Chem. Soc.* **2014**, *136* (46), 16299.
(29) Lu, Z.; Filonov, G. S.; Noto, J. J.; Schmidt, C. A.; Hatkevich, T. L.; Wen, Y.; Jaffrey, S. R.; Matera, A. G. *RNA* **2015**, *21* (9), 1554.
(30) Kellenberger, C. A.; Chen, C.; Whiteley, A. T.; Portnoy, D. A.; Hammond, M. C. *J. Am. Chem. Soc.* **2015**, *137*, 6432−6435.
(31) Nawrocki, E. P.; Burge, S. W.; Bateman, A.; Daub, J.; Eberhardt, R. Y.; Eddy, S. R.; Floden, E. W.; Gardner, P. P.; Jones, T. A.; Tate, J.; Finn, R. D. *Nucleic Acids Res.* **2015**, *43* (D1), D130.
(32) Brueckner, B.; Boy, R. G.; Siedlecki, P.; Musch, T.; Kliem, H. C.; Zielenkiewicz, P.; Suhai, S.; Wiessler, M.; Lyko, F. *Cancer Res.* **2005**, *65* (14), 6305.
(33) Hupkes, M.; Azevedo, R.; Jansen, H.; van Zoelen, E. J.; Dechering, K. J. *J. Biomol. Screening* **2013**, *18* (3), 348.
(34) Xiao, B.; Jing, C.; Wilson, J. R.; Walker, P. A.; Vasisht, N.; Kelly, G.; Howell, S.; Taylor, I. a; Blackburn, G. M.; Gamblin, S. J. *Nature* **2003**, *421*, 652.
(35) Cole, P. A. *Nat. Chem. Biol.* **2008**, *4* (10), 590.
(36) Brescia, P. J. BioTek Appl. note, 2013. http://www.biotek.com/resources/articles/interrogation-set79-histone-lysine-methyltransferase.html.
(37) Zhang, J.-H.; Chung, T. D. Y.; Oldenburg, K. R. *J. Biomol. Screening* **1999**, *4* (2), 67.
(38) Shimizu, S.; Shiozaki, S.; Ohshiro, T.; Yamada, H. *Eur. J. Biochem.* **1984**, *141* (2), 385−392.
(39) Buckstein, M. H.; He, J.; Rubin, H. *J. Bacteriol.* **2008**, *190* (2), 718−726.
(40) Tuerk, C.; MacDougal, S.; Gold, L. *Proc. Natl. Acad. Sci. U. S. A.* **1992**, *89* (15), 6988.
(41) Corbino, K. A.; Barrick, J. E.; Lim, J.; Welz, R.; Tucker, B. J.; Puskarz, I.; Mandal, M.; Rudnick, N. D.; Breaker, R. R. *Genome Biol.* **2005**, *6* (8), R70.
(42) Meyer, M. M.; Roth, A.; Chervin, S. M.; Garcia, G. A.; Breaker, R. R. *RNA* **2008**, *14* (4), 685.
(43) Chames, P.; Van Regenmortel, M.; Weiss, E.; Baty, D. *Br. J. Pharmacol.* **2009**, *157* (2), 220.
(44) Jayasena, S. D. *Clin. Chem.* **1999**, *45* (9), 1628.
(45) McKeague, M.; DeRosa, M. C. *J. Nucleic Acids* **2012**, *2012*, 1.
(46) Klink, T. a; Staeben, M.; Twesten, K.; Kopp, A. L.; Kumar, M.; Dunn, R. S.; Pinchard, C. a; Kleman-Leyer, K. M.; Klumpp, M.; Lowery, R. G. *J. Biomol. Screening* **2012**, *17*, 59−70.
(47) Liu, J.; Yue, Y.; Han, D.; Wang, X.; Fu, Y.; Zhang, L.; Jia, G.; Yu, M.; Lu, Z.; Deng, X.; Dai, Q.; Chen, W.; He, C. *Nat. Chem. Biol.* **2014**, *10* (2), 93.
(48) Deng, X.; Chen, K.; Luo, G.-Z.; Weng, X.; Ji, Q.; Zhou, T.; He, C. *Nucleic Acids Res.* **2015**, *43* (13), 6557.
(49) Roundtree, I. A.; He, C. *Curr. Opin. Chem. Biol.* **2016**, *30*, 46.
(50) Brun, M. A.; Tan, K. T.; Griss, R.; Kielkowska, A.; Reymond, L.; Johnsson, K. *J. Am. Chem. Soc.* **2012**, *134* (18), 7676.
(51) Griss, R.; Schena, A.; Reymond, L.; Patiny, L.; Werner, D.; Tinberg, C. E.; Baker, D.; Johnsson, K. *Nat. Chem. Biol.* **2014**, *10* (7), 598.
(52) Autour, A.; Westhof, E.; Ryckelynck, M. *Nucleic Acids Res.* **2016**, *44* (6), 2491−500.

DOI: 10.1021/jacs.6b01621
J. Am. Chem. Soc. 2016, 138, 7040−7047